We are IntechOpen,
the world's leading publisher of
Open Access books
Built by scientists, for scientists

4,800
Open access books available

122,000
International authors and editors

135M
Downloads

Our authors are among the

154
Countries delivered to

TOP 1%
most cited scientists

12.2%
Contributors from top 500 universities

CLARIVATE ANALYTICS

BOOK CITATION INDEX

INDEXED

WEB OF SCIENCE™

Selection of our books indexed in the Book Citation Index
in Web of Science™ Core Collection (BKCI)

Interested in publishing with us?
Contact book.department@intechopen.com

Numbers displayed above are based on latest data collected.
For more information visit www.intechopen.com

3D-CT Mammary Lymphography Facilitate the Endoscopic Sentinel Node Biopsy

Koji Yamashita, Shunsuke Haga and Kazuo Shimizu
Nippon Medical School
Japan

1. Introduction

In early breast cancer, the presence of metastasis in axillary lymph nodes is an important factor in prognosis and further treatment. However, axillary lymph node dissection causes many complications such as contracture of the shoulder joint, lymph edema, and paralysis of the upper extremities (Ernst, 2002). Convention holds that there is no need to dissect axillary lymph nodes for node-negative patients. To avoid unnecessary axillary lymph node dissection, sentinel node biopsy (SNB) has been performed (Veronesi, 1997; Schrenk, 2000). Sentinel node (SN) is defined as the first lymph node drained of lymph flow from the tumor (Schwartz, 2002; Kuehn, 2005). SNB can detect such metastases and provide information that may obviate the need for axillary lymph node dissection. The most commonly used methods to identify the SN are dye-staining (Giuliano, 1994; Borgstein, 1997) and radioisotope incorporation (Krag, 1993; Giuliano, 1994). Multidetector-row three-dimensional computed tomography (3D-CT) mammary lymphography (LG) can be used to mark the precise location of the SN on the skin before the operation (Suga, 2003; Tangoku, 2004; Minato, 2004).

The detailed relations between lymph nodes and lymph flow in the breast and the axilla can be clarified using 3D-CT LG (Yamashita, 2008, 2009). We have developed this 3D image processing system to depict more precise anatomical structure of mammary lymphovascular system. It enables us to perform systematic collection of axillary lymph nodes including SNs, and will decrease unnecessary lymph node dissection, even if the SNs have metastasized, and can decrease complications.

Previously, we devised an endoscopic surgical procedure for breast diseases; video-assisted breast surgery (VABS) (Yamashita, 2006). VABS is a less invasive and esthetically a better operation for benign and malignant breast diseases In this study, we assessed the validity of 3D-CT LG in SNB of 186 patients, investigated the extent of metastasis style in 40 patients who were metastasis-positive based on the novel technique, and applied the technique to SNB using the dye-staining method and 3D-CT LG guidance.

2. Patients

Since July 2002, SNB was performed in 186 patients, with SNB using VABS and 3D-CT LG being performed in 146 of these. Patient characteristics are shown in Table 1.

	Mean	Range
Age (y/o)	52.7	26 – 85
Tumor size (cm)	2.2	0.1 – 10
	Number	%
Tis	3	1.6
T1a / T1b / T1c	3 / 20 / 86	1.6 / 10.8 / 46.2
T2 / T3 / T4	53 / 9 / 12	28.5 / 4.8 / 6.5
Lymph node metastasis (N)	40	21.5
Distant metastasis (M)	9	4.8
ER (+/-)	122 / 64	65.6
PgR (+/-)	98 / 88	52.7
HER2 (+/-)[a]	44 / 142	23.7
Total	186	

ER, estrogen receptor; PgR, progesterone receptor; HER, human epidermal growth factor receptor
[a] Modified from reference 14.
[b] HER2: human epidermal growth factor receptor type 2; HER2 + means Herceptest 3+ and 2+; HER2 – means Herceptest 1+ and 0

Table 1. Patient Characteristics [a]

3. 3D-CT lymphography

Interstitial 3D-CT LG was performed using a 16-channel multidetector-row helical 3D-CT scanner (Toshiba Aquilion 16; Toshiba Medical Systems Corporation, Tochigi, Japan). Patients were placed in the supine position with arms positioned in the lateral abduction direction, suitable for the operating position. After local anesthesia by subcutaneous injection of 0.5 ml of 1% lidocaine, 2 ml of iopamidol (Iopamiron 300; Nihon Shering, Osaka, Japan) was injected intracutaneously into the periareolar skin and the skin above the tumor. At 1 and 3 min after injection (sometimes 5 min for observing advancement of lymph flow), a CT image was taken with a 3 mm slice thickness. SNs were identified on transaxial CT images, and their location was marked on the skin surface with an oil-painting pen using a laser pointer of CT on the day before the surgery. 3D-CT images were then reconstructed from transaxial enhanced CT images, which clearly showed the lymph ducts and SNs.

4. SPECT

On the day before surgery, 74 MBq technetium 99m (99mTc) phytate (FUJIFILM RI Pharma Co., LTD., Tokyo, Japan) in sterile saline (total volume 1 mL) was injected intradermally into two different sites of the skin above the tumor and around the periareola. Lymphoscintigraphy and SPECT were performed 2 hours after injection of radio colloid. If one or more focal accumulations of radioactivity (hot spots) were visualized, these were assumed to be SNs. Small amount of RI markers were positioned on the jagular notch of sternum and the xiphoid process to correct the fusion points. We used the image fusion software Syntegra (Philips Medical Systems, Eindhoven, The Netherlands) and Real INTAGE (KGT, Tokyo, Japan) to fuse SPECT data with 3D-CT LG.

5. Surgical methods

VABS has been described in detail previously (Yamashita, 2006). The operative procedures were as follows: skin incision in the axilla and/or periareola, skin flap formation via the tunnel method (Yamagata, 2002), pectoral muscle fascia dissection, vertical section of the mammary gland, SNB by the dye-staining method guided by preoperative 3D-CT LG marking, and axillary lymph node dissection (levels I and II). Radiotherapy and chemotherapy were performed for malignant diseases.

SLNB was performed by the dye-staining method using a part of VABS technique at the beginning of the operation, before gland resection. In the periareolar region and over the tumor, 2 ml of 1% indocyanine green was injected subcutaneously. A 1-cm long skin incision was made along wrinkles in the axilla at the position marked by 3D-CT LG. A Visiport optical trocar (Tyco Healthcare Japan, Tokyo, Japan) was inserted into the incision after 20 min. The endoscopic view was observed through Visiport with a 10 mm diameter, straight-angled rigid endoscope (Olympus Optical, Tokyo, Japan), and the stained lymph nodes were found by following the dye in the lymph ducts. The lymph nodes were sampled and metastasis was determined on fast frozen sections. Axillary lymph node dissection was performed at levels I and II with bipolar scissors through the same incision that was lengthened to 2.5 cm. The inferior pectoral nerve, long thoracic nerve, second and third intercostobrachial nerves, thoracodorsal nerve, artery, and vein were observed and preserved. The lateral pectoral artery was preserved for the lateral tissue flap. After surgery, SNs and axillary lymph nodes were pathologically examined by standard H&E staining. Informed consent to the procedure was obtained from all the patients before surgery.

6. Lymph flow from tumor to sentinel node (Yamashita, 2008)

The lymph flow of the whole breast has been reported to collect into a subareolar plexus and then drain towards the axilla via lymph collecting ducts, by human cadaver studies (Delamere, 1993; Standring, 2005). It became the theoretical basis for the subareolar injection of dye and/or isotope for lymphatic mapping as part of the SN biopsy for breast cancer (Kimberg, 1999; Kern, 1999). On the other hand, the individual lymphatic flow is not identical in each living patient studies of SN biopsy.

3D-CT LG showed the precise lymphatic flow from the tumor to the SN (Fig. 1). In Figure 1a, the lymphatic flow from the tumor was divided to the periareola and directly to the axilla. The periareolar lymphatic flow was draining from the tumor and circling around the nipple and went to the axilla. This lymph duct to the axilla was separated from the direct duct from the tumor. In Figure 1b, the lymphatic flow was multiple and complicated, but the basic structure was same as that of Fig. 1a.

We classified the relationship between the lymph ducts and drained SNs into four patterns (Yamashita, 2008) (Fig. 2), according to the classification by Suga et al. (Suga, 2005). A single duct to single node pattern was observed in 88 cases (60.2%), multiple ducts to a single node in 29 cases (19.9%), single duct to multiple nodes in two cases (1.4%), and multiple ducts to multiple nodes in 27 cases (18.5%).

The internal mammary SN was also detected in five patients, but the rate was lower than that of the peritumoral injection (Shimazu, 2003). We are trying to improve it by the injection of the contrast medium iopamidole into the retromammary space behind the tumor. The peritumoral injection, which is recommended in radioisotope technique, is not

suitable for 3D-CT LG, because the contrast medium is needed to use much volume as 1 ml and it may flow into surrounding mammary duct systems.
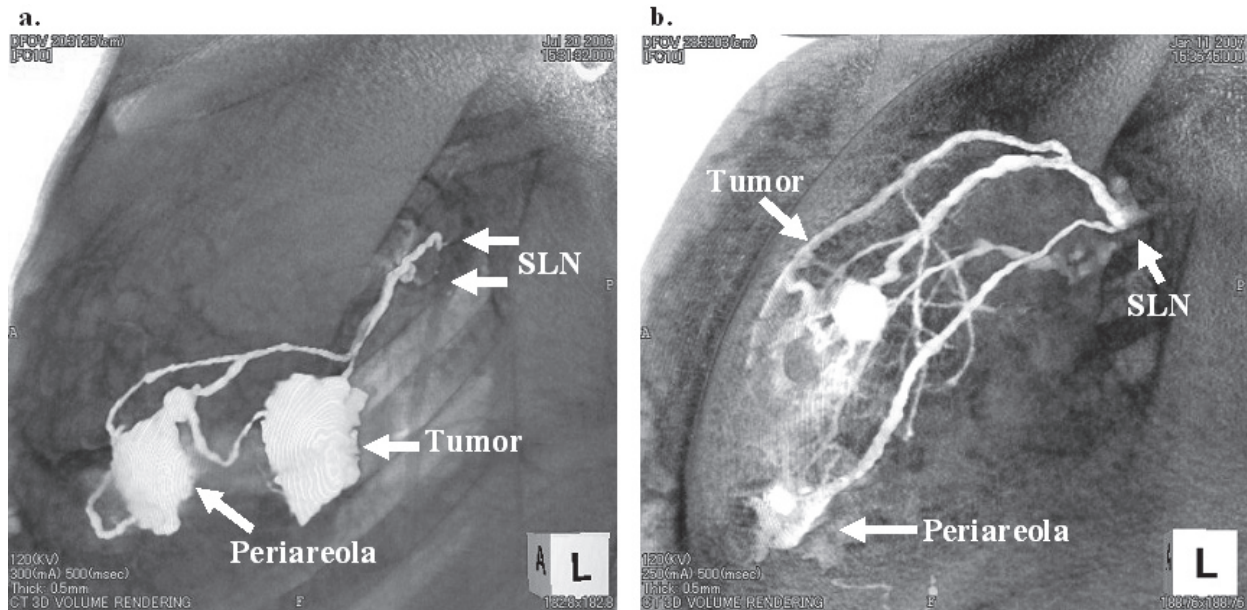

Fig. 1. Visualization of SNs and lymph ducts (LD) using 3D-CT LG *(13)*.
Iopamidol was injected intracutaneously into the periareolar skin and the skin above the tumor. a) Two LDs draining into two SNs. b) Multiple LDs draining into a single SN.
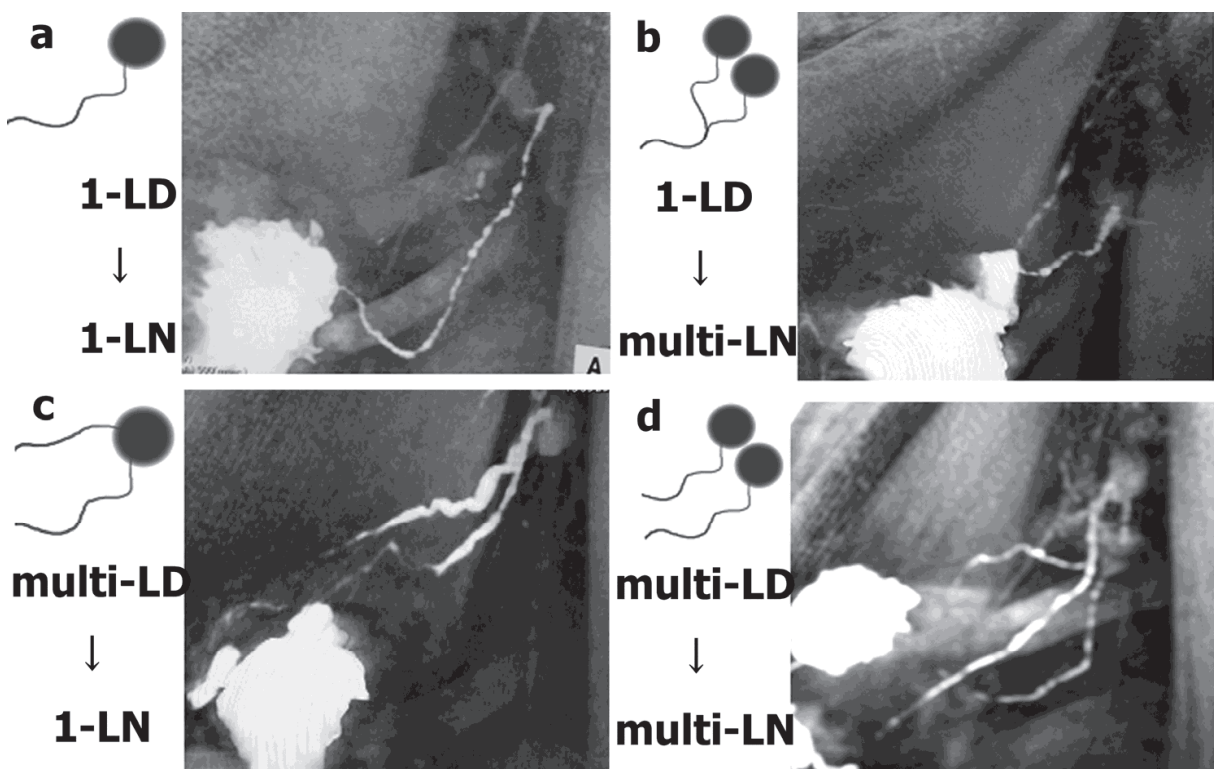

Fig. 2. Four patterns of relationship between the lymph duct and the sentinel lymph node (Yamashita, 2009).
The lymph flow pattern can be classified into these four types.

SN is typically detected using dye-staining or radioisotope incorporation. However, the tract from the tumor to the SN cannot be observed clearly by either methods (Mariani, 2001; Giuliano, 1997). We cannot detect whether dye-stained or hot-spotted nodes are really the first lymph nodes. This may be the basis for false negatives in SN biopsy. Lymphoscintigraphy may only show the main negative lymph node, and cannot clearly visualize the direct connection of SN and their afferent lymph ducts, because of slow lymphatic migration of radiocolloids, and because of the limitation of spatial resolutions and the lack of anatomic landmarks. In contrast, 3D-CT LG can demonstrate the precise route of the lymph duct and the exact location of the SN with the detailed surrounding anatomic structures, and since it does not involve the use of radioisotopes, it can be done at any institution that is equipped with a CT scanner. Therefore, 3D-CT LG is a very useful examination, which is essential for SNB.

Interstitial injection of iopamidol had no adverse effects locally and generally. The pathological metastatic status of SNs and axillary lymph nodes was as follows. No SN was identified in five patients of the 40 SNBs using only the dye-staining method, and the detection rate was 87.5%. However, all SNs were identified in 146 SNBs using the dye-staining method with 3D-CT LG marking. This detection rate was 100%. Backup axillary dissection was performed in each of the 40 SNB patients in the early phase according to both methods of SNB. One false-negative case occurred only in the dye-staining method (12.5%), but no false-negative case was found in 3D-CT LG (0%). The average sampled number of SNs was 1.7 in the cases without 3D-CT LG and 2.3 in the cases with 3D-CT LG.

Four patterns of lymph ducts and SNs have been revealed using 3D-CT LG (Yamashita, 2008). The lymph ducts to the SN are complicated. For example, in this study, we observed that in over 60% of cases, many ducts joined together into a single duct to form a single SN. However, more than two SNs were shown in 19.9% of the cases. These may have been missed without 3D-CT LG guidance. Figure 4a shows a typical example of a multi-node pattern, in which three different lymph nodes were all SN, each from a different lymph duct. The node from the main thick duct was not metastasized; however, the other two from the narrow collateral duct were metastasized. Thus, the sampling of all three nodes is necessary. The dye-staining method and the isotope method of SNB could not reach such the latter collateral nodes. These might become false negative study. Therefore, 3D-CT LG is effective in raising accuracy of SNB.

7. Lymph flow from sentinel node to axillary angle in axilla (Yamashita, 2009)

The procedure of 3D-CT LG takes only about 1 min after injection of iopamidol subcutaneously over the tumor and around the nipple for representing SN precisely. Examination of iopamidol flow 1, 3, and 5 min after injection revealed that the flow extended over the SN into the next nodes, and into the venous angle in half of the patients examined. Therefore, we can easily ascertain the tracts that cancer cells will spread through during metastasis. We defined these tracts as the second and third SNs. As a representative example, Fig. 3 shows a clear view of five bead-like grouped lymph nodes beyond the SN into the center of the body, and lymph duct plexuses between them. They are thought to imply the order of lymphatic route of metastasis. Fig. 4a shows three separated SNs, which were drained from three different lymph ducts diverging from one duct. Two of three separated SNs were positive for metastasis, but the other SNs from the main lymph duct were negative. Fig. 4b shows two chained SNs. The first SN was positive for metastasis, but the second was negative.
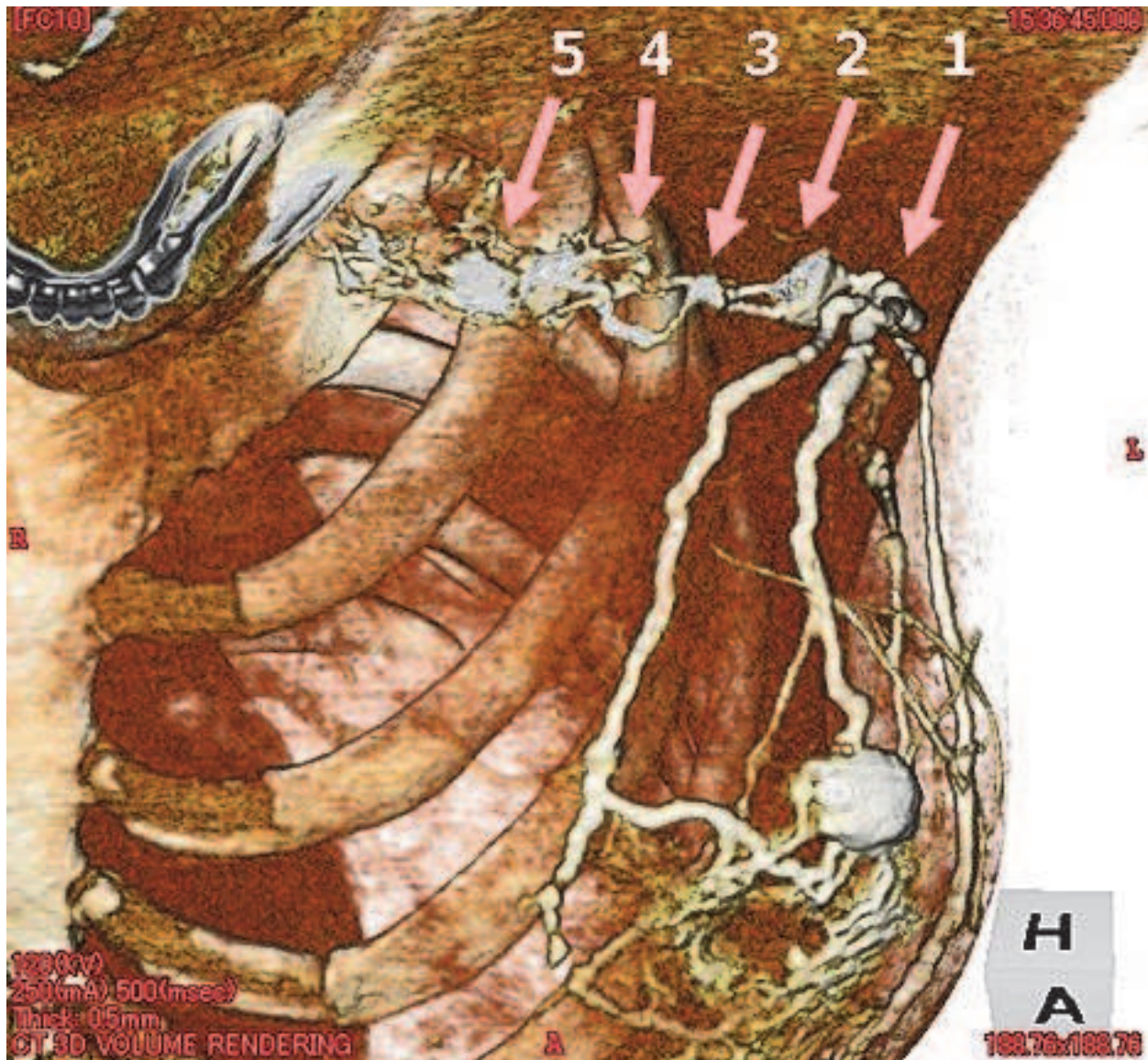
Fig. 3. Chronological examination of 3D-CT LG (Yamashita, 2009).
3D-CT LG was examined 1, 3, and 5 min after iopamidol injection. Iopamidol flowed to extend over the SN into the next nodes. Five bead-like grouped lymph nodes in the axilla can be visualized by partially removing the pectoral muscle in the CT monitor.
These are thought to be the order of lymph metastasis. Arrows point to lymph nodes 1–5 after SN.

Since December 2001, we performed VABS in 230 patients, SN biopsy in 186 patients, and 3D-CT LG in 140 patients. Table 2 shows the pathological status of metastases in SNs and axillary lymph nodes. SN metastasis was positive in 40 patients; of these, 21 patients experienced metastases solely in the SN. Except for SN, only the second axillary lymph node group was metastasized in three patients, the second and the third node groups were metastasized in five patients, and more than three groups were metastasized in eleven patients. It was confirmed that these metastases occurred in order of lymph flow presented by the lymphoid path of these 3D-CT LG (Fig. 3, 4).
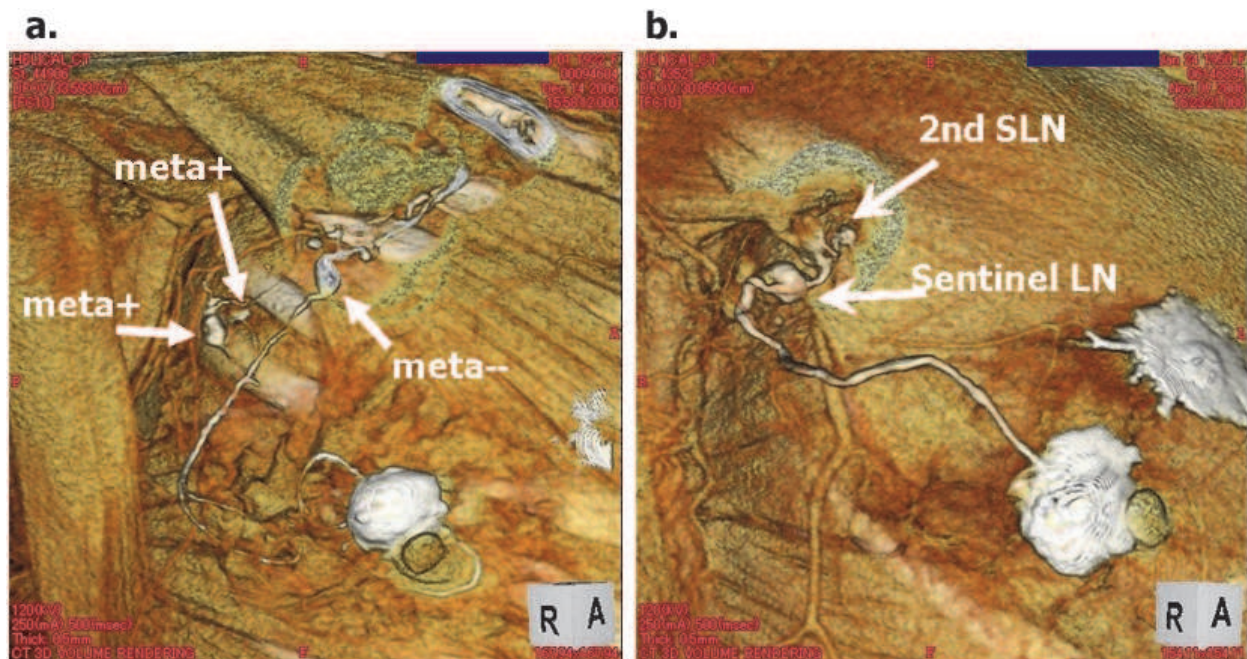
Fig. 4. Detection of SN metastasis (Yamashita, 2009).
a) Three sentinel nodes are recognized by 3D-CT LG. The right node drained from the main lymph duct was not metastasized. On the other hand, the other two nodes drained from the narrow collateral duct were metastasized. Dye and isotope could not reach such the latter collateral nodes. These might become false negative study. Therefore, 3D-CT LG is effective in raising accuracy of SNB.
b) The sentinel node was metastasized, but the second node and the other nodes were all negative.

The second and third lymph nodes groups could be recognized by 3D-CT LG and selectively removed by VABS. Table 2 shows the pathological status of their metastases and the other axillary lymph nodes in 40 SN metastasized patients. If second and third lymph node group biopsy was performed, it was prognostic for other axillary lymph node metastasis. Its accuracy, sensitivity, and false negative rate were 100%, 100%, and 0%, respectively.

Status of 2nd and 3rd Sentinel LN metastasis		Status of Axillary LN metastasis*	
		Negative	Positive
Positive	19	8	11
Negative	21	21	0
Total	40	29	11

Table 2. Metastatic relations of 2nd and 3rd SN to the other axillary nodes [a]
LN: lymph node
* Number of Axillary LN metastasis: Primary, and 2nd, and 3rd Sentinel LN is not included.
2nd and 3rd Sentinel LN biopsy: Accuracy = 100 %, False negative rate = 0 %, Sensitivity = 100 %

Even if the patients presently examined had metastasis of SN, about half of them had no metastasis in axillary lymph nodes (21 among 40 patients, 52.5% in Table 3). In these patients presenting with only SN metastasis, sufficient information can be obtained regarding the lymph node status of cancer staging to plan primary therapy after surgery, avoiding axillary lymph node dissection. Since the absence of other metastases is crucial to this approach, we need to analyze how it would be possible to conclude that SLN metastasis is unique. We suggest that this can be confirmed by collecting lymph nodes systemically based on the 3D-CT LG-acquired map of lymph nodes and ducts beyond SN. Histological examination of fast-frozen sections of the second and third lymph nodes during the operation will provide the information to omit axillary lymph node dissection.

Sentinel LN metastasis		No. of Axillary LN metastasis*			
		2nd	3rd	$4^{th}<$	Sum
Positive	40	19	16	11	19
Negative	141				
Not detected	5	0	0	0	0
Total	186	19	16	11	19

Table 3. Metastatic status of sentinel and the other axillary nodes
[a] Detection rate 97.3% (without 3D-CT 88% / 40, with 3D-CT 100% /146
 Average LN number 2.0, Only SLN metastasis 21 (52.5%)
LN: lymph node, 3D-CT: 3-dimensional computed tomography, LG: lymphography
* Axillary LN metastasis: Sentinel LN is not included*

8. Metastatic evaluation by 3D-CT LG

3D-CT LG may predict whether SN is metastasizing or not. When occupied with cancer cells, 3D-CT LG shows only the trumpet-like inflow portion of the lymph node, but the node is still recognizable. Sometimes, the lymph duct detours around the metastasized lymph node. However, in partial metastasis of the lymph node, 3D-CT LG shows no apparent difference from normal nodes. We have to examine the pattern of the duct route and the enhanced pattern of lymph node more carefully to predict metastasis. Ultrasonography and magnetic resonance imaging show only morphology and blood flow, and cannot reveal metastasis. While positron emission tomography can detect some metastases, those that are small escape detection. Of all these techniques, 3D-CT LG is superior.

9. Endoscopic SNB guided by 3D-CT LG

We have performed endoscopic surgery, named as video-assisted breast surgery (VABS), for all breast surgical procedures through a small wound port in the inconspicuous axillary area or periareola (Yamashita 2006a, 2006b). VABS is also used for SNB. The incisional wound is only 1 cm long and inconspicuous, without any complications. However, precise information is needed about the location of SN, because the method relies on endoscopic

vision. In five cases, we could not find the SLN using just only the dye-staining method. 3D-CT LG guidance helps in finding the SN easily by giving precise information. The structure of the dye-stained lymph ducts and SN were exactly the same on the endoscopic view as with the 3D-CT LG.

The lymph ducts to the SN are complicated. In most cases, many ducts join together into a single duct to a single SN (60.6 %). However, more than two SNs were shown in 19.7%, and these may have been missed without 3D-CT LG guidance, and hence 3D-CT LG is indispensable for SNB.

10. SPECT-CT

SPECT-CT can show the exact location of the hot spots on the axial view of the CT image, as showing in the figure (Fig. 5). They are always coincided with the axillary nodes. However, it cannot show the lymph ducts and the relations between lymph ducts and nodes either. The number of hot spots was usually only one or two. The average number was 1.2, which was less than the number 2.3 of SN found by 3D-CT LG.
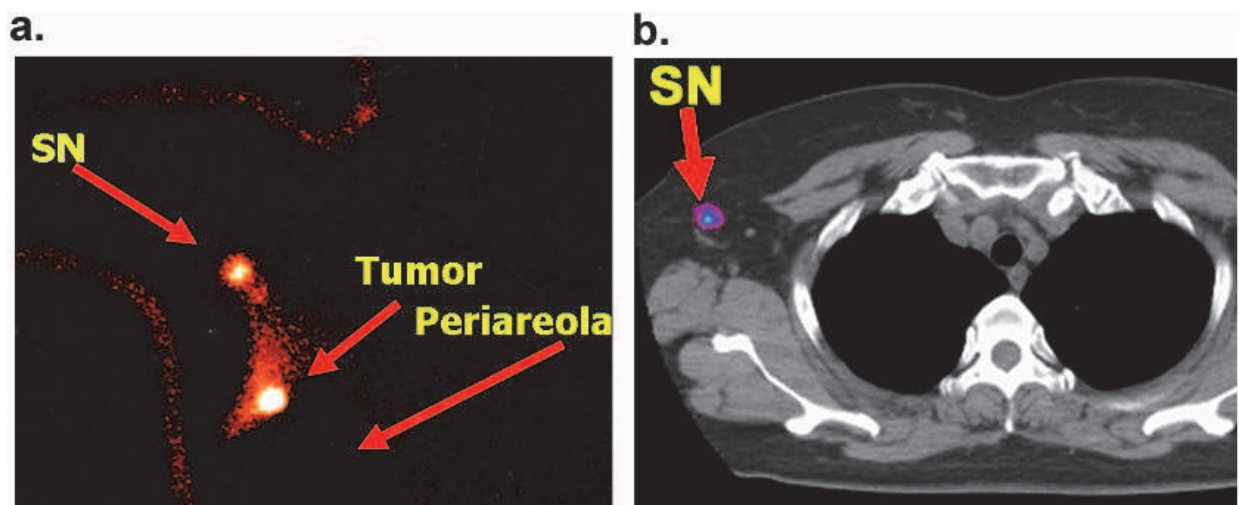

Fig. 5. Lymphoscintigraphy and SPECT-CT
a. Lymphoscintigraphy
The conventional lymphoscintigraphy shows only information about the existence of nodes with an uptake of RI as hot spots
b. Single photon emission computed tomography (SPECT)
SPECT-CT can show the exact location of the hot spots on the axial view of the CT image, as showing in the figure. They are always coincided with the axillary nodes.
SN: sentinel node

We fused the DICOM data of SPECT with 3D-CT LG by using the image fusion software (Fig. 6). The hot spot can be coincided with enhanced SN observed on 3D-CT LG. However, not all of SNs had a hot spot. We call SN with a hot spot as a hot node and SN without a hot spot as a cold node. We can recognize the location of the cold nodes by using the relation to the hot nodes on the map of 3D-CT LG.
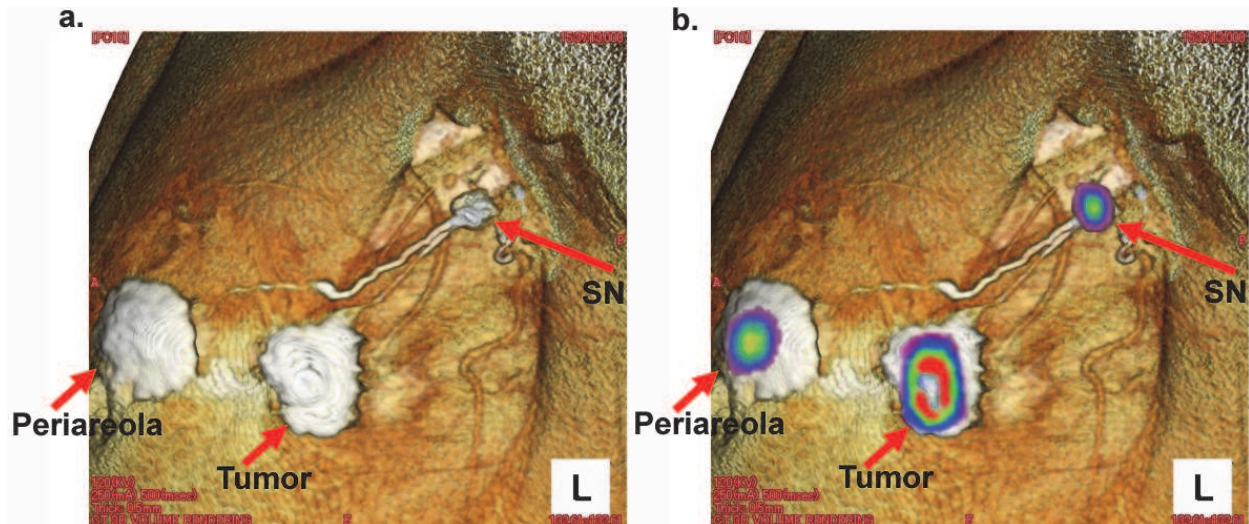
Fig. 6. 3D-CT lymphography and SPECT-fused 3D-CT LG
a. 3D-CT lymphography (LG)
The contrast enhancing materials flow from the injected sites over the tumor and the periareola through the two lymph ducts into single SN in the axilla.
b. SPECT-fused 3D-CT LG
DICOM data of SPECT was projected on 3D-CT LG. The hot spots were coincided with SN detected by 3D-CT LG.

11. Conclusion

By 3D-CT LG, we can recognize the accurate and more precise lymph flow in the breast and the axilla. Even in patients with SN metastasis, if we find no metastatic presence in the second and third SN, the need to dissect more nodes is obviated. In the near future, it will be necessary to omit axillary dissection in such patients.

12. References

Ernst MF, Voogd AC, Balder W. (2002). Early and late morbidity associated with axillary level I-III dissection in breast cancer. *J Surg Oncol*, 79, pp. 151–5.

Veronesi U, Paganelli G, Galimberti V. (1997). Sentinel-node biopsy to avoid axillary dissection in breast cancer with clinically negative lymphnodes. *Lancet*, 349, pp. 1864–7.

Schrenk P, Rieger R, Shamiyeh A. (2000). Morbidity following sentinel lymph node biopsy versus axillary lymph node dissection for patients with breast carcinoma. *Cancer*, 88, pp. 608–14.

Schwartz GF, Giuliano AE, Veronesi U. (2001). Proceedings of the consensus conference on the role of sentinel lymph node biopsy in carcinoma of the breast April 19 to 22, 2001, Philadelphia, Pennsylvania. *Cancer*, 94, pp. 2542–51.

Kuehn T, Bembenek A, Decker T. (2000). A Concept for the Clinical Implementation of Sentinel Lymph Node Biopsy in Patients with Breast Carcinoma with Special Regard to Quality Assurance. *Cancer*, 103, pp. 451–461.

Giuliano AE, Kirgan DM, Guether V. (1994). Lymphatic mapping and sentinel lymphadenectomy for breast cancer. *Ann Surg*, 220, pp. 391–8.

Borgstein PJ, Meijer S, Pijpers R. (1997). Intradermal blue dye to identify sentinel lymph-node in breast cancer. *Lancet*, 384, pp. 149–57.

Krag DN, Weaver DL, Alex JC. (1993). Surgical resection and radiolocalization of the sentinel lymph node in breast cancer using a gamma probe. *Surg Oncol*, Vol.2, No. 6, pp. 335–9.

Giuliano AE, Kirgan DM, Guenther JM. (1994). Lymphatic mapping and sentinel lymphadenectomy for breast cancer. *Ann Surg*, Vol.220, No.3, pp. 391–8.

Suga K, Ogasawara N, Okada M. (2003). Interstitial CT lymphography-guided localization of breast sentinel lymph node: preliminary results. *Surgery*, 133, pp. 170–179.

Tangoku A, Yamamoto S, Suga K. (2004). Sentinel lymph node biopsy using computed tomography-lymphography in patients with breast cancer. *Surgery*, 135, pp. 258–265.

Minato M, Hirose C, Sasa M. (2004). 3-Dimensional computed tomography lymphography-guided identification of sentinel lymph node in breast cancer patients using subcutaneous injection of nonionic contrast medium. A clinical trial. *J Comput Assist Tomogr*, 28, pp. 46–51.

Yamashita K, Shimizu K. (2008). Video-assisted Breast Surgery and Sentinel Lymph Node Biopsy guided by 3D-CT lymphography. *Surg Endosc*, 22, pp. 392-397

Yamashita K, Shimizu K. (2009). Evaluation of sentinel lymph node metastasis alone guided by three-dimensional computed tomographic lymphography in video-assisted breast surgery. *Surg Endosc*, 2008; DOI 10.1007/s00464-008-9809-z. 23, pp. 633–640, 2009

Yamashita K, Shimizu K. (2006). Endoscopic Video-Assisted Breast Surgery: Procedures and Short-Term Results. *J Nippon Med Sch*, 73, pp. 193–202.

Yamagata M, Takasugi T, Takayama T. (2002). Partial mastectomy by the periareolar incision. *Geka Chiryo*, 86, pp. 932–940.

Delamere G, Poirier P, Cuneo B. (1903). The lymphatics. In: Charpy PP eds. A trearise of human anatomy. Westminster: Archibald Constable.

Susan Standring (2005), Editor in Chief, Gray_s Anatomy: The Anatomical Basis of Clinical Practice. 39th Ed. Elsevier Churchill Livingstone.

Kimberg VS, Rubio IT, Henry R, et al. (1999). Subareolar versus peritumoral injection for location of the sentinel node. *Am Surg*, 6, pp. 860–5.

Kern KA. (1999). Sentinel lymph node mapping in breast cancer using subareolar injection of blue dye. *J Am Coll Surg*, 189, pp. 539–45.

Suga K, Yamamoto S, Tangoku A, Oka M. (2005). Breast sentinel lymph node navigation with three-dimensional multidetector-row computed tomographic lymphography. *Invest Radiol*, 40, pp. 336–342.

Shimazu K, Tamaki Y, Taguchi T, et al. (2003). Lymphoscintigraphic visualization of internal mammary nodes with subtumoral injection of radiocolloid in patients with breast cancer. *Ann Surg*, 237, pp. 390–8.

Mariani G, Moresco L, Viale G. (2001). Radioguided sentinel lymph node biopsy in breast cancer surgery. *J Nucl Med*, 42, pp. 1198–1215.

Giuliano AE, Jones RC, Brennan M. (1997). Sentinel lymphadenectomy in breast cancer. *J Clin Oncol*, 15, pp. 2345–2350.

Yamashita K, Shimizu K. (2006). Video-Assisted Breast Surgery: Reconstruction More than 33% Resected Breast. *J Nippon Med Sch*, 73, pp. 320-327.
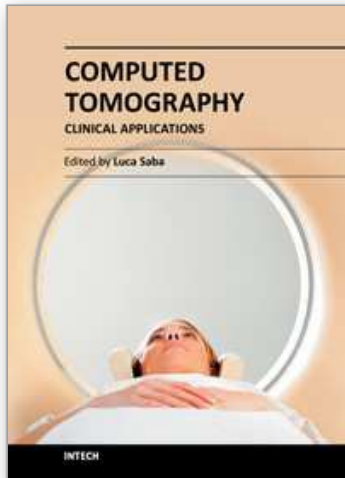
Computed Tomography - Clinical Applications

Edited by Dr. Luca Saba

Computed Tomography (CT), and in particular multi-detector-row computed tomography (MDCT), is a powerful non-invasive imaging tool with a number of advantages over the others non- invasive imaging techniques. CT has evolved into an indispensable imaging method in clinical routine. It was the first method to non-invasively acquire images of the inside of the human body that were not biased by superimposition of distinct anatomical structures. The first generation of CT scanners developed in the 1970s and numerous innovations have improved the utility and application field of the CT, such as the introduction of helical systems that allowed the development of the "volumetric CT" concept. In this book we want to explore the applications of CT from medical imaging to other fields like physics, archeology and computer aided diagnosis. Recently interesting technical, anthropomorphic, forensic and archeological as well as paleontological applications of computed tomography have been developed. These applications further strengthen the method as a generic diagnostic tool for non- destructive material testing and three-dimensional visualization beyond its medical use.

How to reference

In order to correctly reference this scholarly work, feel free to copy and paste the following:

Koji Yamashita, Shunsuke Haga and Kazuo Shimizu (2012). 3D-CT Mammary Lymphography Facilitate the Endoscopic Sentinel Node Biopsy, Computed Tomography - Clinical Applications, Dr. Luca Saba (Ed.), ISBN: 978-953-307-378-1, InTech, Available from: http://www.intechopen.com/books/computed-tomography-clinical-applications/3d-ct-mammary-lymphography-facilitate-the-endoscopic-sentinel-node-biopsy

INTECH
open science | open minds